materials proceedings

Proceeding Paper

Factors Affecting the Properties of Slag-Based Alkali-Activated Materials †

Konstantinos Komnitsas [1,*], Vasiliki Karmali [1], Dimitra Vathi [1] and Eleftherios Kaklamanos [2]

[1] School of Mineral Resources Engineering, Technical University of Crete, 73100 Chania, Greece; vkarmali@tuc.gr (V.K.); dvathi@tuc.gr (D.V.)
[2] Euronickel, 1430 Kavadarci, North Macedonia; lefteris.kaklamanos@euronickel.com
* Correspondence: kkomnitsas@tuc.gr; Tel.: +30-28210-37686

† Presented at the 2nd International Conference on Raw Materials and Circular Economy "RawMat2023", Athens, Greece, 28 August–2 September 2023.

Abstract: This study, carried out in the frame of the Horizon Europe ENICON project, "Sustainable processing of Europe's low grade sulphidic and lateritic Ni/Co ores and tailings into battery grade metals", evaluates the properties of alkali-activated materials (AAMs) produced from slag obtained from the Euronickel ferronickel plant at Kavadarci, Republic of N. Macedonia. The activating solution comprises sodium hydroxide (NaOH) and sodium silicate (Na_2SiO_3) solutions. The effect of various operating parameters, i.e., the molarity of the activating solution (6–10 mol/L), pre-curing period (24–96 h), curing temperature (20–80 °C), and aging period (7–96 days) on the compressive strength, density, porosity and water absorption of the produced AAMs, was initially assessed. The first experimental results indicate that the produced AAMs acquired compressive strength exceeding 40 MPa after curing at 80 °C and aging for 7 days. This value increased to higher than 55 and 70 MPa when the aging period was 28 and 96 days, respectively.

Keywords: ferronickel; slag; Kavadarci; compressive strength

check for updates

Citation: Komnitsas, K.; Karmali, V.; Vathi, D.; Kaklamanos, E. Factors Affecting the Properties of Slag-Based Alkali-Activated Materials. *Mater. Proc.* **2023**, *15*, 19. https://doi.org/10.3390/materproc2023015019

Academic Editors: Antonios Peppas, Christos Roumpos, Charalampos Vasilatos and Anthimos Xenidis

Published: 24 October 2023

1. Introduction

Metallurgical industries generate millions of tons of slags annually. Even though they are used in different applications in various industrial sectors, including the cement and concrete industry, their improper disposal may cause adverse environmental impacts [1,2]. With this in mind, alkali activation is an alternative and low-cost technology that can be used for the valorization of metallurgical slags and the production of alkali-activated materials (AAMs) [3,4]. AAMs are inorganic polymers that exhibit beneficial physical, mechanical, and thermal properties and may find numerous applications in the construction industry. Their production requires precursors rich in Si and Al, alkaline solutions, relatively low curing temperature (30–90 °C), and a short aging period [5,6]. This experimental study aims to identify the optimal alkali-activation conditions for the production of slag-based AAMs.

2. Materials and Methods

The precursor used in this study is Euronickel slag (ENS) produced in the ferronickel plant at Kavadarci, Republic of N. Macedonia. Prior to use, ENS was dried at 80 °C for 1 day, pulverized using a Fritsch-BICO pulverizer (Fritsch, Dresden, Germany), and characterized for its chemical and mineralogical composition. Its particle size analysis was determined using a Mastersizer S (Malvern Instruments) analyzer. The chemical composition in the form of oxides was determined with the use of a Bruker S2 Ranger energy-dispersive X-ray fluorescence spectrometer (ED-XRF, Bruker, Karlsruhe, Germany), while the mineralogical analysis was performed using an X-ray diffractometer (Bruker AXS, D8-Advance, Bruker, Karlsruhe, Germany) with a Cu tube, a LynxEye detector with a Ni filter and scanning range from 4° to 70° 2theta (2θ), a step size of 0.02°, and 0.4 s/step measuring time.

Qualitative analysis was carried out using the DiffracPlus Software (EVA v. 4.2, Bruker, Karlsruhe, Germany) and the Crystallographic Open Database (COD database), while for the quantitative determination of mineralogical phases, the Rietveld software AutoQuan v.2.8 (Seifert GE) was used. FTIR analysis was carried out on KBr pellets with a PerkinElmer 1000 spectrometer (PerkinElmer, Akron, OH, USA) in the range of 400 to 4000 cm^{-1}. For the production of the pellets, slag was mixed with KBr at a ratio of 1:100 w/w.

Regarding the synthesis of AAMs, the ground slag was mixed with the alkaline solution, consisting of NaOH and Na_2SiO_3 solutions, for about 10 min. The liquid-to-solid ratio was kept low and varied between 0.19 and 0.23, while the mass of each component was (wt%): slag 78%, 10 M NaOH solution 11%, and Na_2SiO_3 solution 11%. The paste was cast in cubic steel molds $5 \times 5 \times 5$ cm^3, while after the initial hardening, the specimens were de-molded and heated at 20–80 °C in an oven (ON-02G) for 24 h. After curing, the specimens were left at room temperature for 7, 28, and 96 days. All measurements were carried out in triplicate. The compressive strength of the produced AAMs was determined using the MST 815 (1600 KN) rock mechanics test system with a loading rate of 0.5–1 MPa/s, whereas the other physical properties of selected AAMs were determined in accordance with BS EN 1936 (2006) [7].

3. Results and Discussions

3.1. Characterization of ENS

The main chemical composition, in the form of oxides, and the particle size of ENS are presented in Table 1.

Table 1. Chemical composition (wt%) and particle size of ENS.

Chemical Composition	**wt%**
SiO_2	37.8
Al_2O_3	4.3
Fe_2O_3	31.5
MgO	17.4
CaO	4.7
Particle size	**µm**
d_{90}	34.4
d_{50}	4.4
d_{10}	0.3

The mineralogical analysis of ENS, as derived using XRD, is presented in Figure 1. The main mineralogical phases identified are olivine [$(Mg,Fe)_2SiO_4$] 16 wt%, plagioclase [$NaAlSi_3O_8$–$CaAl_2Si_2O_8$] 9 wt%, fayalite [Fe_2SiO_4] 28 wt%, diopside [$CaMgSi_2O_6$] 13 wt%, magnetite [Fe_3O_4] 2 wt%, and magnesiochromite [$MgCr_2O_4$] 2 wt%, while its amorphous content is 30 wt%.

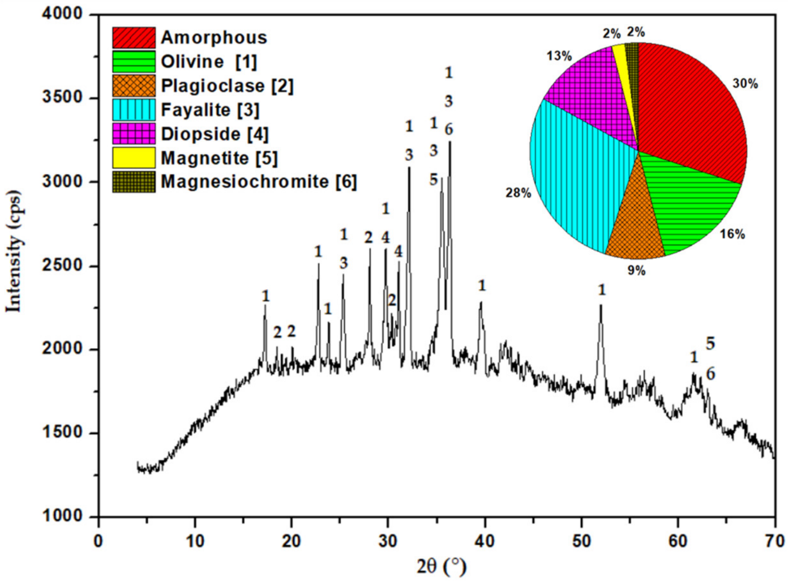

Figure 1. XRD pattern and mineralogical composition of ENS.

3.2. Alkali Activation of ENS

Figure 2 shows the compressive strength of AAMs produced using different NaOH concentrations (6–10 M) and curing temperatures (20–80 °C) after an aging period of 7 days. The SiO_2/Na_2O molar ratio in the activating solution was kept at 1, while the pre-curing and curing periods were 24 h.

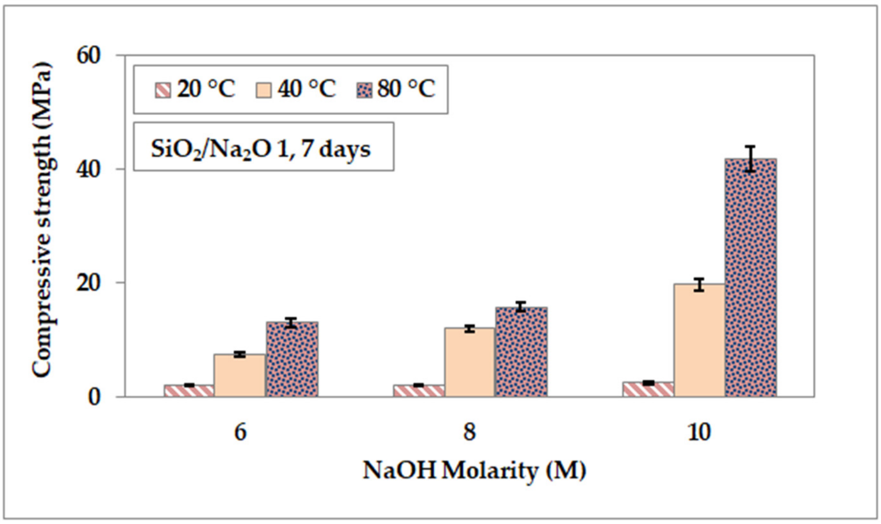

Figure 2. Effect of NaOH concentration and curing temperature on the compressive strength of ENS-based AAMs (error was calculated from measurements of three specimens).

It can be seen that the AAMs produced with the use of 10 M NaOH obtained the highest compressive strength (41.8 MPa) after curing at 80 °C, as indicated in earlier studies [8]. These AMMs also exhibited the lowest porosity (4.9%) and water absorption (1.9%) and the highest density (2.7 g cm^{-3}).

Figure 3 shows the effect of the aging period on the compressive strength of ENS-based AAMs produced under optimum conditions. It can be seen that when the aging period increases from 7 to 96 days, the compressive strength increases by almost 75% (from 41.8 MPa to 73.6 MPa).

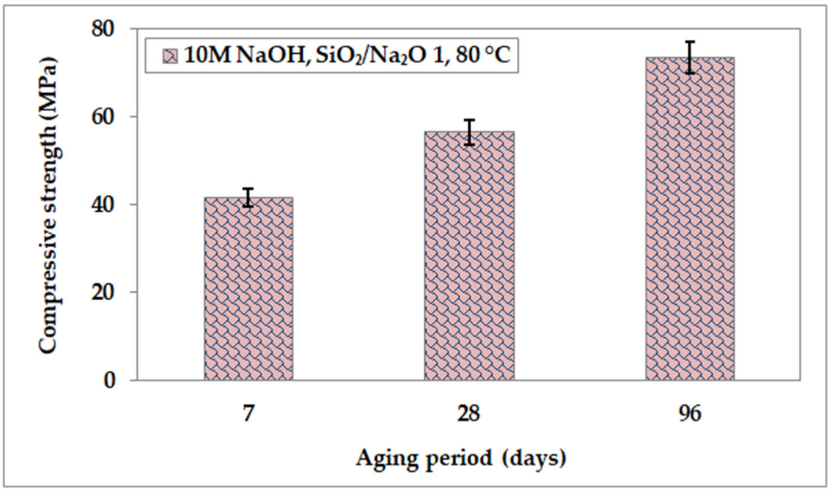

Figure 3. Effect of aging period on the compressive strength of ENS-based AAMs (error was calculated from measurements of three specimens).

4. Characterization of Selected AAMs

Figure 4 shows the FTIR spectra of ENS and the AAM with a compressive strength of 41.8 MPa produced under the following conditions: 10 M NaOH, pre-curing and curing times of 24 h, curing temperature of 80 °C, and aging period of 7 days.

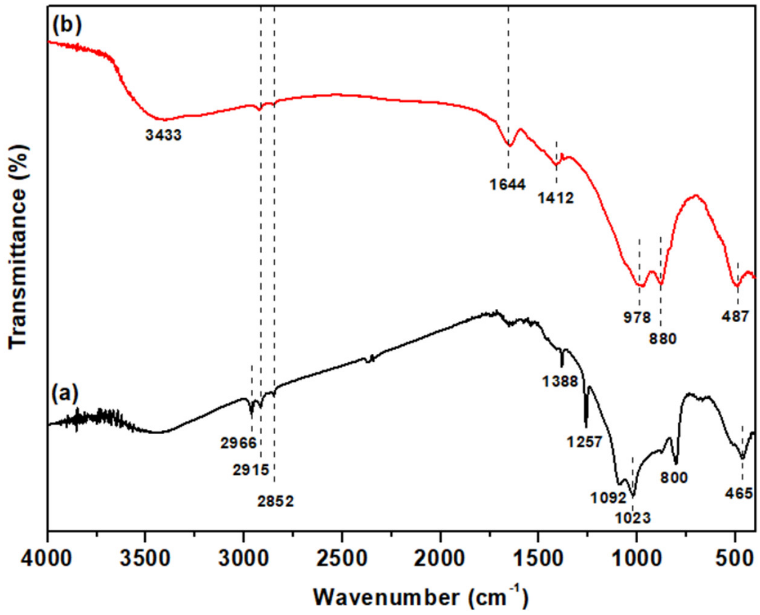

Figure 4. FTIR spectra of (**a**) ENS slag and (**b**) AAM with a strength of 41.8 MPa.

First, the band seen at 465 cm^{-1} in ENS corresponds to symmetric bending Si–O, while the bands observed at 800, 1023, 1092, and 1257 cm^{-1} are attributed to the asymmetric stretching vibration of Si–O–T bonds (T = Si or Al) [9,10]. Furthermore, the broad band seen at 1388 cm^{-1} denotes the presence of water due to bending vibrations of O–H bonds. The band at 2966 cm^{-1} is attributed to stretching and bending H–O–H vibrations of bound water molecules [8].

In the produced AAMs, new characteristic bands are observed. The band seen at 487 cm^{-1} is attributed to the overlapping Si-O-Si and O-Mg-O bending vibrations, whereas the band at 978 cm^{-1} is assigned to the asymmetric stretching of Si-O-T bonds (T = Fe, Al, or Si) [11]. The bands at 880 cm^{-1} and 1412 cm^{-1} are assigned to the anti-symmetric stretching and out-of-plane bending modes of $CO_3{}^{2-}$ ions. In addition, the bands at

~3430 cm^{-1} and ~1650 cm^{-1} denote stretching (O–H) and bending (H–O–H) vibrations of water, respectively [12].

5. Conclusions

The present study investigated the alkali activation potential of ENS. The produced AAMs achieved the highest compressive strength (73.6 MPa) when the synthesis conditions were: molarity of 10 M NaOH, curing temperature of 80 °C, pre-curing and curing periods of 24 h, and aging period of 96 days. As a result, alkali activation appears to be a promising alternative for the valorization of large volumes of slag and the production of binders or construction materials.

Author Contributions: K.K. carried out the conceptualization, methodology, supervision, review, and editing. V.K. carried out the experiments and prepared the original draft. D.V. carried out the experiments. E.K. provided the material and carried out review and editing. All authors have read and agreed to the published version of the manuscript.

Funding: This research was funded by the Horizon Europe ENICON project, "Sustainable processing of Europe's low grade sulphidic and lateritic Ni/Co ores and tailings into battery grade metals" at https://enicon-horizon.eu/ (accessed on 16 August 2023).

Institutional Review Board Statement: Not applicable.

Informed Consent Statement: Not applicable.

Data Availability Statement: The data presented in this study are available on request from the corresponding author. The data are not publicly available at this moment because the report to the funding authority is pending.

Conflicts of Interest: The authors declare no conflict of interest.

References

1. Bai, T.; Song, Z.G.; Wu, Y.G.; Hu, X.D.; Hua, B. Influence of steel slag on the mechanical properties and curing time of metakaolin geopolymer. *Ceram. Int.* **2018**, *44*, 15706–15713. [CrossRef]
2. Komnitsas, K.; Zaharaki, D.; Perdikatsis, V. Geopolymerisation of low calcium ferronickel slags. *J. Mater. Sci.* **2007**, *42*, 3073–3082. [CrossRef]
3. Davidovits, J. Geopolymers—Inorganic polymeric new materials. *J. Therm. Anal. Calorim.* **1991**, *37*, 1633–1656. [CrossRef]
4. Hertel, T.; Pontikes, Y. Geopolymers, inorganic polymers, alkali-activated materials and hybrid binders from bauxite residue (red mud)-Putting things in perspective. *J. Clean. Prod.* **2020**, *258*, 120610. [CrossRef]
5. Komnitsas, K.; Zaharaki, D. Geopolymerisation. A review and prospects for the minerals industry. *Miner. Eng.* **2007**, *20*, 1261–1277. [CrossRef]
6. Bernal, S.A.; de Gutierrez, R.M.; Provis, J.L.; Rose, V. Effect of silicate modulus and metakaolin incorporation on the carbonation of alkali silicate-activated slags. *Cem. Concr. Res.* **2010**, *40*, 898–907. [CrossRef]
7. *BS EN 1936:2006*; Natural Stone Test Methods. Determination of Real Density and Apparent Density and of Total and Open Porosity. BSI (British Standards Institute): London, UK, 2007.
8. Zaharaki, D.; Galetakis, M.; Komnitsas, K. Valorization of construction and demolition (C&D) and industrial wastes through alkali activation. *Constr. Build. Mater.* **2016**, *121*, 686–693. [CrossRef]
9. Iacobescu, R.I.; Cappuyns, V.; Geens, T.; Kriskova, L.; Onisei, S.; Jones, P.T.; Pontikes, Y. The influence of curing conditions on the mechanical properties and leaching of inorganic polymers made of fayalitic slag. *Front. Chem. Sci. Eng.* **2017**, *11*, 317–327. [CrossRef]
10. Nikolov, A.; Karamanov, A. Thermal Properties of Geopolymer Based on Fayalite Waste from Copper Production and Metakaolin. *Materials* **2022**, *15*, 2666. [CrossRef] [PubMed]
11. Traven, K.; Češnovar, M.; Ducman, V. Particle size manipulation as an influential parameter in the development of mechanical properties in electric arc furnace slag-based AAM. *Ceram. Int.* **2019**, *45 Pt B*, 22632–22641. [CrossRef]
12. Li, Q.; Yang, Y.; Yang, K.; Chao, Z.; Tang, D.; Tian, Y.; Wu, F.; Basheer, M.; Yang, C. The role of calcium stearate on regulating activation to form stable, uniform and flawless reaction products in alkali-activated slag cement. *Cem. Concr. Res.* **2019**, *103*, 242–251. [CrossRef]